ASIAN JOURNAL OF CIVIL ENGINEERING (BUILDING AND HOUSING) VOL. 8, NO. 4 (2007)
PAGES 443-458

BEHAVIOUR OF SINGLE PILE UNDER LATERAL CYCLIC LOAD IN MARINE CLAY

S. Basack[*a] and R.D. Purkayastha[b]
[a]Bengal Engineering and Science University, Shibpur, Howrah-711 103, India
[b]Jadavpur University, Kolkata-700 032, India

ABSTRACT

The subject of pile foundation subjected to lateral cyclic load is an age-old problem confronted by Geotechnical Engineers. The environment prevalent in ocean necessitates the piles supporting offshore and onshore structures to be designed against lateral cyclic loading resulting from the effects of sea waves. Such loading induces remarkable deterioration in the interactive performance of the soil-pile system. This can be manifested as significant loss in pile capacity associated with increased pile head deflection. The work reported herein is aimed towards conducting extensive experimental investigation on model pipe pile in marine clay under lateral cyclic loading, subsequently followed by theoretical analysis using finite difference technique. The experimental results are compared with the theoretical results and reasonably good agreement is noted. This paper presents brief description of the experimentation and theoretical analysis carried out with some typical results and the relevant conclusions drawn therefrom.

Keywords: Amplitude, cyclic loads, degradation, finite difference method, lateral loads, marine clays, pile foundation.

1. INTRODUCTION

Offshore and onshore structures, namely, quay and harbour structures, jetties, tension leg platforms, oil drilling platforms, etc. are largely supported on pile foundations. Apart from usual loads from superstructures, these piles are subjected to continuous action of wave loading. This type of lateral loading is quasi-static cyclic in nature. It results in considerable degradation in the interactive performance of the pile-soil system causing progressive reduction in pile capacity associated with increased pile-soil stiffness. This may ultimately lead to disastrous consequences.

Amongst limited research works in this field, the major contributions are made by Matlock [1], Idriss et al. [2], Poulos [3], Vucetic et al. [4] and Basack [5]. A brief review of these works indicates that the degradation of the pile-soil system under lateral cyclic loading

[*] Email-address of the corresponding author: basackdrs@hotmail.com

mainly depends upon the following parameters : number of cycles, frequency (cycles per unit time), cyclic load level (ratio of cyclic load amplitude to the lateral static ultimate pile capacity, in case of load-controlled mode) and cyclic displacement level (ratio of cyclic displacement amplitude applied at the pile head to the external pile diameter, in case of displacement-controlled mode). As pointed out by Poulos [6-7], the degradation is mainly due to partial to zero dissipation of excess pore water pressure generated during cyclic loading in progress, destruction of inter-particle bond with particle realignment & rearrangement and gradual accumulation of irrecoverable plastic deformation around the pile.

Usually, cohesive marine soil exists in coastal regions. So the entire investigation is aimed towards a detailed study of single, vertical pile embedded in marine clay, under two-way symmetrical lateral cyclic loading. The work consists of extensive laboratory experimentations followed by rigorous theoretical analysis.

2. TYPES OF LATERAL CYCLIC LOADING

Lateral cyclic load applied on pile head may be classified as one-way and two-way loadings. In case of one-way lateral cyclic loading, the load is cycled in any particular direction and hence it varies between maximum and minimum values along the same direction. In case of two-way cyclic loading, on the other hand, the applied cyclic load alternates in either direction about a certain mean value. When this mean value is zero, it is termed as symmetrical two-way cyclic loading, otherwise unsymmetrical. All the above types of lateral cyclic loading may be under load-controlled mode or displacement-controlled mode. In former case, the load applied at the pile head varies cyclically with time such that its maximum and the minimum values remain constant for all cycles. In the later case, it is the pile head deflection and not the applied load, which varies cyclically with time such that its maximum and the minimum values remain constant for all cycles.

3. EXPERIMENTATION

The experimentation consists of sophisticated testing under controlled conditions. Since ready apparatus is not available, a multipurpose set-up has been designed and fabricated.

3.1 Test Set Up

The experimental set up mainly consists of motor-gear arrangements associated with cam mechanism, crank-shaft mechanism and other mechanical components. A sketch showing the basic principle of the apparatus is depicted in Figure 1. A typical photographic view is presented in Figure 2. The entire set up consists of the following primary components : test tank, loading device, pile head connector and other ancillary equipments.

3.2 Test Tank

A cylindrical stainless steel tank having 600 mm internal diameter, 760 mm clear height and

5 mm wall thickness has been used for preparing the test bed. It may be split longitudinally into three equal flanged segments, which can be bolted one above the other. To provide water tightness, 5 mm thick rubber gaskets are provided between adjacent flanges. The entire tank is rested on screw jacks which are fixed to the floor.

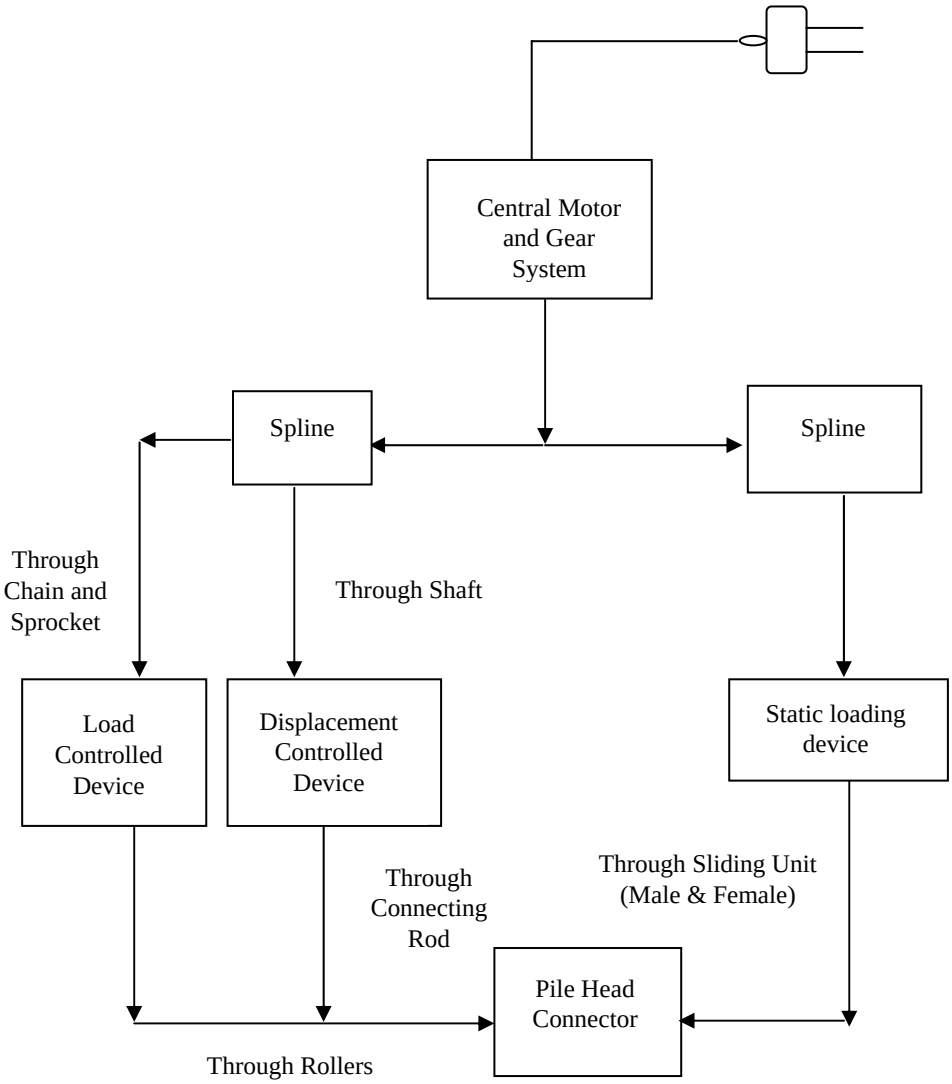

Figure 1. Basic operating principle of the cyclic loading device.

3.3 Loading Device

The loading device may be sub-divided into three components, viz., central motor-gear system, static loading device and cyclic loading device.

The lateral static and cyclic loads are applied on the pile head at different rates by means of central motor-gear system. A 2 H.P., reversible, induction type of motor equipped with star-delta connection is the main driving unit. The speed of motor is reduced firstly by a

reduction gear-box so that various frequencies are obtained by different pairs of detachable spur gears.

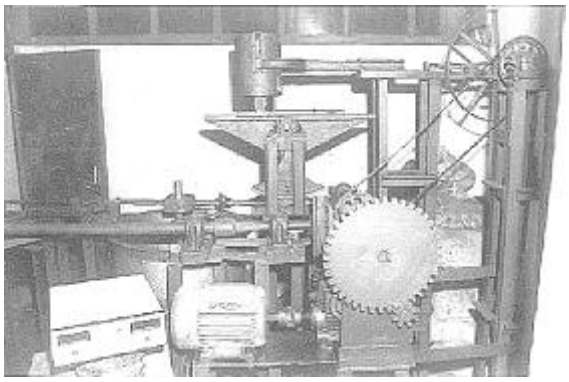

Figure 2. Photographic view of the apparatus

In order to perform pre-cyclic and post-cyclic lateral static pile load tests, the model pile is pushed forward steadily at a constant rate of horizontal advancement. This purpose is served by incorporating worm gear mechanism between the pile head connector and the output point of the central motor-gear system. By measuring the horizontal pile head deflection and the corresponding applied lateral load, the load-displacement response can be plotted, which ultimately yields the static lateral capacity of pile.

The cyclic loading device consists of two sub-components: load-controlled and displacement-controlled devices. The three components of loading device are connected in parallel between the motor-gear system and the pile head connector such that one unit can be operated at a time.

A symmetrical two-way lateral cyclic load, for a specified number of cycles at a specified frequency with a specified cyclic load level, is applied at the pile head by the load-controlled device. As shown in Figure 3, it consists of an oscillating arm supported on a pin-joint 'O'. A semi-circular pinion is welded at the base of this arm, which is connected to a rack arm whose other end is fixed to the pile head connector. A movable weight W slides on the top of the arm sinusiodally by means of crank-shaft mechanism, keeping the joint 'O' at mean. The axial reaction R by the pinion on the rack at any instant 'τ' may be obtained statically as,

$$R = (Wx_0 / h) \sin 2\pi f\tau \qquad (1)$$

where, x_0 is the maximum value of x, the horizontal displacement of W from 'O'. Thus, the amplitude of cyclic load is given as, $R_{max} = Wx_0 / h$. Adequate altering of W yields different values of cyclic load levels. It has been observed from load cell readings that the actual cyclic load amplitude is about 10% less than its theoretical value and also the pattern of variation of the applied lateral cyclic load with time deviates slightly from its exact sinusoidal nature. Understandably this is due to irregular frictional resistances.

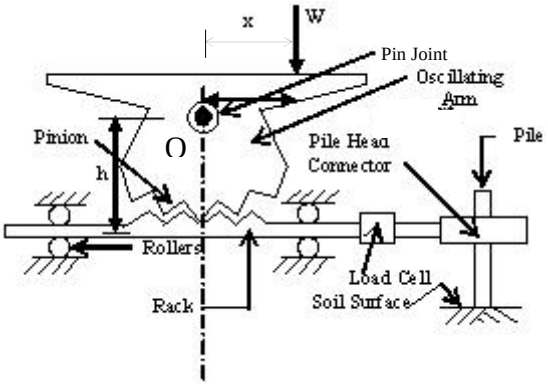

Figure 3. Basic principle of the load-controlled device.

The displacement-controlled device, on the other hand, imparts symmetrical two-way sinusoidal pile head deflection by means of cam mechanism. To obtain different cyclic displacement levels, cam shafts having various eccentricities are used.

3.4 Pile Head Connector

Components of loading device are connected to the pile head via load cell by means of pile head connector, which is specially designed to provide both the free and the fixed pile head conditions. As observed from Figure 4, the pile passes through a collar clamped by bolts with balls attached at their ends to ensure lateral fixity of the pile without eliminating its freedom for axial movement. With the help of the arrangements made by the pairs of swinging screw and fixing screw, required pile head conditions can be obtained. Without the fixing screws, the pile head is free to rotate, and vice versa.

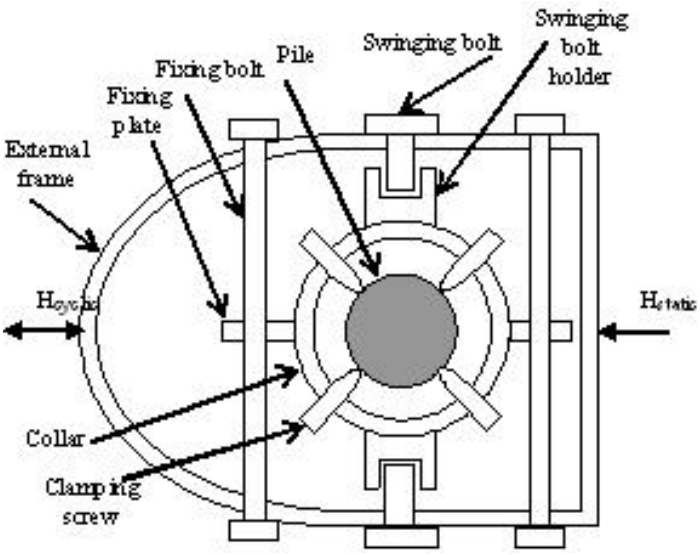

Figure 4. Pile head connector.

3.5 Ancillary Equipments

To measure the lateral loads applied on the pile head connector, two load cells, one for static load and the other for cyclic load, are used. The pile head deflection is measured with a dial gauge connected to the front face of the pile head connector. The number of cycles are registered in a digital counter attached to the spur gear shaft. To install the model pile vertically and centrally into the prepared soil bed, a special pile driving machine equipped with rack-pinion arrangement is manufactured. It can be bolted on the test tank prior to pile installation and can be detached later.

3.6 Soil

Soft marine clay collected from a depth of about 12 m at the dockyard area of Visakhapattanam port, India has been used for preparing the remoulded test bed. The soil consists of 60% clay, 27% silt and 13% sand, as obtained from hydrometer test. The Atterberg Limits are reported as 9%, 47% and 16% respectively. The specific gravity of soil particles is 2.62. From Standard Proctor compaction test, the marine clay has been found to have a maximum dry density of 14.3 kN/m^3 at an optimum moisture content of 32%. Chemical analysis of the marine clay indicates a pH of 7.2, organic matter content of 7.24%, exchangeable ferrous ion content of 0.005%, carbonate content of 22.63% and cation exchange capacity of 30.8 meq/100 gm of soil. The U.U. triaxial tests of saturated samples taken from various depths of the prepared test bed indicate the average values of c_u and ϕ as 22.5 kN/m^2 and 4° respectively, with the initial tangent modulus as 10 MN/m^2.

3.7 Model Pile

Both the instrumented and non-instrumented piles are used. Hollow cylindrical stainless steel pipes having 30 mm external diameter and 5 mm wall thickness are used as model pile. The depth of embedment is 600 mm. The lateral load is imparted from a height of 100 mm above the soil surface. To insert the pile easily through the soil bed, a conical shoe of stainless steel is welded at its tip. The instrumented pile, in addition, is split longitudinally into two equal halves. A cap and the conical shoe can be tightened at the opposite ends. To ensure water tightness, rubber gasket is provided on wall sections. Starting from the tip, seven electronic strain gauges are fixed at the inner face of pile @ 100 mm c/c.

3.8 Test Procedure

Experiments are done sequentially with the following steps:

(i) Marine clay samples, saturated at a moisture content of 54%, is filled in six equal layers within the test tank, each layer being compacted by hammering technique. Thereafter, the model pile is installed centrally and vertically within the test bed. The pile head connector is then attached to the pile head. (ii) By engaging the static loading device only, the pre-cyclic static test is conducted. The test bed should be re-prepared after completion of this test. (iii) According to the requirement, either load-controlled or displacement-controlled cyclic loading device is attached to the pile head connector. Appropriate spur gear set should then be engaged to obtain desired frequency. The required cyclic load or displacement levels are also adjusted. (iv) Motor is started. At the completion of desired number of cycles, it is stopped. (v) The pile is once again tested for lateral static loading to

assess its post cyclic performance. (vi) For each test, separate test bed is to be prepared.

4. THEORETICAL ANALYSIS

The method suggested by Poulos [3,7] has been followed as a preliminary guideline with relevant modifications. Analysis is carried out using finite difference technique.

4.1 Assumptions

The entire theory is based upon the following assumptions: (i) The subsoil is a homogeneous, isotropic, semi-infinite, initially elastic-perfectly plastic material. When elastic, it has a constant Young's modulus (E_s) and Poisson's ratio which remain unaffected by the presence of the pile. (ii) The pile behaves as an elastic beam. (iii) Possible horizontal shear stresses between the soil and the sides of pile are ignored. (iv) The soil strictly adheres to the pile surface. (v) Pile tip is free to translate and rotate.

4.2 Pile under Lateral Static Load

The idealized problem is depicted in Figure 5. The single, vertical pile has been idealized as a thin vertical plate of width 'd', length 'L' and flexural rigidity 'E_pI_p'. Lateral static load 'H' is applied from a height of 'e' above G.L. The embedded portion of the pile is longitudinally discretized into finite number of elements each having equal length except the two extreme ones which are of half the length of others. In case of the free headed pile, a clockwise moment is applied at the pile head in addition. Any i-th pile element is subjected to a lateral soil pressure p_i which is assumed to act uniformly over the surface of the entire element. The primary objective is to evaluate the displacements of the soil and the pile at the central nodal points of each element and to apply displacement compatibility.

The soil displacements are obtained by integrating the equation of Mindlin [8] over each elements. The expressions already obtainable from the works of Douglas & Davis [9] is utilized for this purpose. The nodal displacements of the idealized pile are evaluated by expressing the standard fourth order differential equation of an elastic beam in finite difference form. The horizontal load and moment equilibrium equations are considered as well. By displacement compatibility, the nodal displacements of the soil and that of the pile should be equal. These nodal displacements are therefore replaced by the unknown soil pressures. The final expression is written in matrix form as,

$$[C] \{ p \} = \{D\} \tag{2}$$

where, [C] is a square matrix termed as coefficient matrix, {p} is the soil pressure vector and {D} is the relevant augment vector. Solving this equation, {p} is obtained.

The elastic soil pressures p_i are then compared with a specific yield pressure p_{iu} for that i-th element. If $| p_i | \geq | p_{iu} |$, the element is assumed to have been failed, and p_i is replaced by p_{iu}. The soil pressures for the remaining unfailed elements are determined. The entire procedure is then recycled until for all elements, $| p_i | \leq | p_{iu} |$. The value of p_{iu} is considered as : $2c_u$ at G.L., increasing linearly upto a depth of 3d to a constant value of $9c_u$, the value

being maintained for remaining greater depths. This assumption is in accordance with Broms [10].

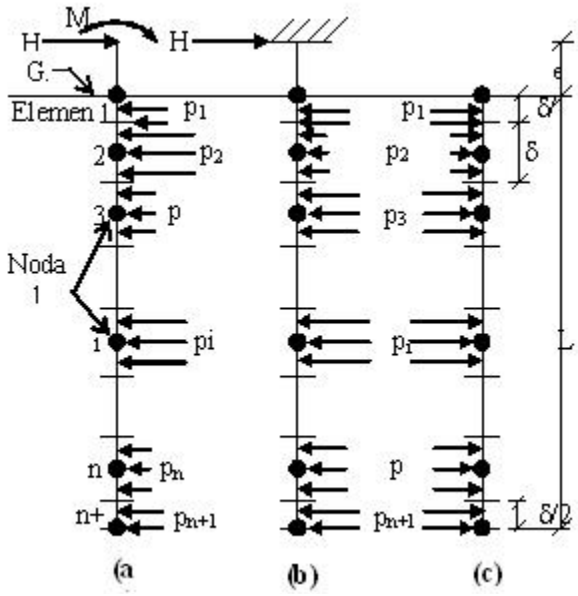

Figure 5. Stresses acting on (a) free headed pile. (b) fixed headed pile.
(c) soil adjacent to pile surface

After determination of {p}, the nodal displacements ρ_i are obtained by backfiguring in the pile displacement relations. The expressions for pile head deflection ρ_h, evaluated by considering the flexure equation of pile above G.L., are obtained as,

$$\rho_h = \rho_1(1+e/\delta)-\rho_2\,(e/\delta)+e\delta\,(M+He)/(2E_pI_p) + (3M+2He)e^2/(6E_pI_p) \quad \text{[Free headed pile]....(3a)}$$

$$\rho_h=\rho_1+He^3/(3E_pI_p)+e^2\delta^2 d\{0.5(p_1+p_{n+1})+(p_2+p_3+\ldots p_n)\}/(2E_pI_p) \quad \text{[Fixed headed pile]...(3b)}$$

Nodal bending moments and shear forces are found out by considering the equilibrium of the portion of pile below G.L. To determine the ultimate lateral capacity of pile, the value of H is increased stepwise. The load corresponding to which all the pile elements fail or the maximum nodal bending moment or shear force exceeds the limiting values, whichever is less, is considered to be the ultimate lateral capacity.

4.3 Pile under Lateral Cyclic Load

The post cyclic response of pile is governed by two opposing phenomena : degradation of p_{iu} and E_s at the nodal points and the effect of loading rate. The degradation of soil strength and stiffness has been quantified by a term degradation factor D_{si}, which is defined as the post-cyclic to pre-cyclic values of nodal soil strength and stiffness. As stated by Idriss et al. [2], for soft cohesive soil, $D_{si} = N^{-t}$, where, N is the number of cycles and t is denoted as

degradation parameter, a unique function of α_i , the cyclic strain amplitude at i-the nodal point. In accordance with Vucetic et al. [4], for marine clay, $t = \alpha_i / (A + B\ \alpha_i)$, where, 'A' & 'B' are arbitrary constants, whose values depend upon the marine clay in particular and should be determined experimentally by either Cyclic Undrained Triaxial (CyUT) or Cyclic Undrained Direct Simple Shear (CyUDSS) tests. The value of α_i is numerically equal to one-sixth the nodal displacement per unit pile diameter, in accordance with Poulos [7].

The undrained strength and stiffness of cohesive soil increases increases linearly with logarithm of loading rate, according to Poulos [7]. Mathemetically, the nodal rate factor may be written as, $D_{ri} = 1 + F \log_{10}(\lambda_i / \lambda_d)$, where, λ_i is the nodal strain rate, λ_d is a datum strain rate and 'F' is an arbitrary constant termed as rate factor, to be determined experimentally from U.U. triaxial test.

The combined nodal soil degradation factor, thus, may be formulated as,

$$D_i = [1 + F \log_{10}(\lambda_i / \lambda_d)]\ [N]\ -\alpha_i / (A + B\ \alpha_i) \tag{4}$$

The value of λ_i is estimated as its average value for one quarter cycle. Thus,

$$\lambda_i = 4\ f\ \alpha_i \tag{5}$$

where, f is the frequency of cyclic loading.

4.4 Method of Computation

The sequential steps of computation are presented below:

(i) From the initial input parameters for soil, pile and loading, static analysis is carried out. The unknown lateral soil pressures and nodal displacements are found out. (ii) The combined nodal soil degradation factors are calculated and the new values of p_{iu} and E_{si} are evaluated. (iii) Steps (i) & (ii) above are recycled until desired convergence is achieved. (iv) The degradation factor D_f for ultimate lateral capacity of pile, defined as the ratio of its post-cyclic to pre-cyclic values, is calculated.

4.5 Development of Computer Software

As may be observed, the entire analysis is based upon iterative technique. A user-friendly computer software LSPIN (Lateral Soil Pile Interaction) is developed to carry out the computations.

5. RESULTS AND DISCUSSIONS

For theoretical analysis, the values of A & B are reasonably assumed [Figure 6] as per Vucetic et al. [4]. From a series of U.U. triaxial tests, F is calculated as 0.01. The value of λ_d is chosen at the rate corresponding to of 6 mm/min.

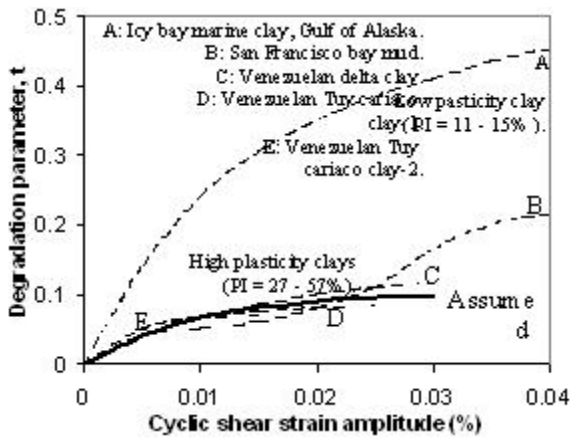

Figure 6. Variation of degradation parameter with cyclic shear strain amplitude for different marine clays

5.1 Lateral Load Deflection Response and Ultimate Lateral Capacity

Both for the experimental and theoretical cases, the applied lateral loads are observed to increase with pile head deflection in hyperbolic manner, the load being stabilized to its optimum value with the head deflection of about 25% to 35% pile diameter. This stabilized value is considered as the ultimate capacity. The experimental and the theoretical ultimate capacities are obtained as 78Kg and 76Kg for free headed pile and 178 Kg & 176 Kg for fixed headed pile respectively. The experimental and the theoretical degradation factors (D_f) are presented in Table 1. The average variation between experimental and theoretical degradation factors has been noted to be of about 4%, the experimental values being on the higher side.

5.2 Variation of D_f with N and f

It is observed that the general tendency of D_f is to decrease with N and increase with f and asymptotically tends to a constant value. Two representative plots are shown in Figures 7 and 8, respectively.

5.3 Variation of D_f with Cyclic Load and Displacement Levels

D_f is observed to decrease with increasing cyclic load and displacement levels. The reduction is non-linear, but not asymptotic. Two representative plots are shown in Figures 9-10, respectively.

5.4 Bending Moment Diagram of Pile

Typical experimental and theoretical bending moment diagrams, one for free headed and the other for fixed headed piles are shown in Figure 11(a,b) respectively. For free headed pile, the bending moment gradually increases from zero at the head to a maximum value at some depth below G.L. after which it again decreases to zero at the tip. Also, the depth of maximum bending moment increases with pile head deflection. In case of fixed headed pile, on the other hand, the bending moment is observed to attain its maximum negative value at head. It then increases to zero at some depth below G.L., further increases to a maximum

positive value and thereafter decreases to zero at the tip. In both cases, the magnitude of maximum bending moment reduces with increasing number of cycles. Also, the average variation of the absolute theoretical and experimental maximum bending moments lies between 1-5%, the theoretical value being on the higher side.

Table 1. Values of degradation factors

Pile head condition	**Number of cycles**	**(A) Load-controlled mode: Cyclic load level: 15.00% Frequency (c.p.m.*)**			**22.35% Frequency (c.p.m.)**			**30.00% Frequency (c.p.m.)**		
		10	**25**	**35**	**10**	**25**	**35**	**10**	**25**	**35**
Free headed pile	100	0.897#	0.920	0.931	0.869	0.905	0.921	0.841	0.882	0.896
		0.862$	*0.884*	*0.895*	*0.834*	*0.873*	*0.886*	*0.809*	*0.847*	*0.858*
	500	0.850	0.890	0.903	0.805	0.840	0.856	0.765	0.803	0.816
		0.817	*0.856*	*0.868*	*0.773*	*0.811*	*0.824*	*0.736*	*0.772*	*0.783*
	1000	0.829	0.869	0.882	0.779	0.814	0.829	0.718	0.754	0.766
		0.797	*0.836*	*0.848*	*0.747*	*0.785*	*0.797*	*0.690*	*0.725*	*0.735*
Pile head condition	**Number of cycles**	**Cyclic load level: 7.16% Frequency (c.p.m.*)**			**10.67% Frequency (c.p.m.)**			**14.33% Frequency (c.p.m.)**		
		10	**25**	**35**	**10**	**25**	**35**	**10**	**25**	**35**
Fixed headed pile	100	0.929	0.958	0.967	0.917	0.942	0.950	0.906	0.928	0.939
		0.893	*0.919*	*0.928*	*0.882*	*0.906*	*0.913*	*0.871*	*0.892*	*0.902*
	500	0.907	0.934	0.943	0.940	0.910	0.917	0.870	0.903	0.919
		0.872	*0.896*	*0.905*	*0.850*	*0.875*	*0.882*	*0.853*	*0.886*	*0.900*
	1000	0.897	0.923	0.933	0.883	0.896	0.903	0.855	0.893	0.910
		0.862	*0.888*	*0.895*	*0.849*	*0.862*	*0.895*	*0.822*	*0.859*	*0.875*
Pile head condition	**Number of cycles**	**(B) Displacement-controlled mode: Cyclic displacement level: 3.33% Frequency (c.p.m.*)**			**5.00% Frequency (c.p.m.)**			**6.67% Frequency (c.p.m.)**		
		10	**25**	**35**	**10**	**25**	**35**	**10**	**25**	**35**
Free headed pile	100	0.844	0.880	0.888	0.822	0.853	0.867	0.804	0.837	0.847
		0.815	*0.848*	*0.858*	*0.791*	*0.820*	*0.834*	*0.773*	*0.803*	*0.816*
	500	0.779	0.811	0.819	0.745	0.762	0.775	0.699	0.737	0.745
		0.752	*0.784*	*0.792*	*0.719*	*0.733*	*0.745*	*0.683*	*0.711*	*0.720*
	1000	0.754	0.783	0.789	0.703	0.730	0.741	0.690	0.711	0.719
		0.725	*0.757*	*0.766*	*0.676*	*0.702*	*0.713*	*0.663*	*0.674*	*0.684*
Fixed headed pile	100	0.891	0.900	0.901	0.867	0.898	0.913	0.849	0.883	0.892
		0.857	*0.856*	*0.866*	*0.834*	*0.864*	*0.878*	*0.818*	*0.849*	*0.858*
	500	0.802	0.835	0.843	0.765	0.793	0.806	0.741	0.771	0.780
		0.771	*0.803*	*0.812*	*0.736*	*0.763*	*0.775*	*0.714*	*0.741*	*0.750*
	1000	0.764	0.797	0.806	0.725	0.751	0.763	0.697	0.727	0.734
		0.735	*0.766*	*0.775*	*0.697*	*0.722*	*0.734*	*0.671*	*0.699*	*0.706*

*c.p.m. means cycles per minute; # normal font means experimental values; $ italized font means theoretical values.

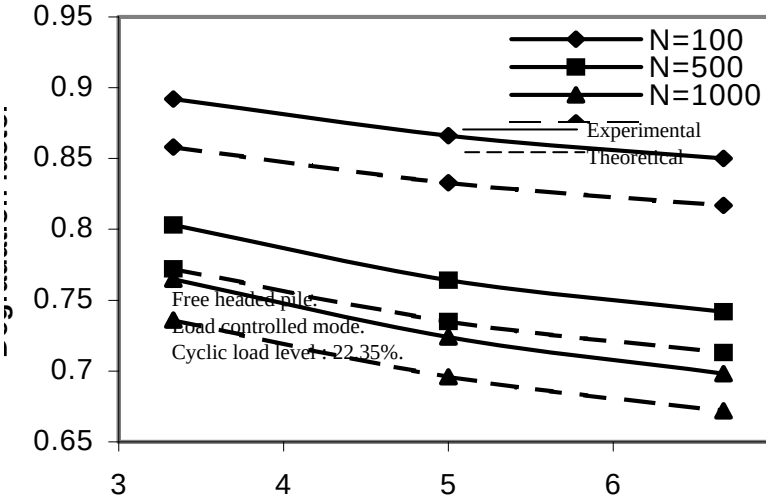

Figure 7. Typical variation of degradation factor with number of cycles

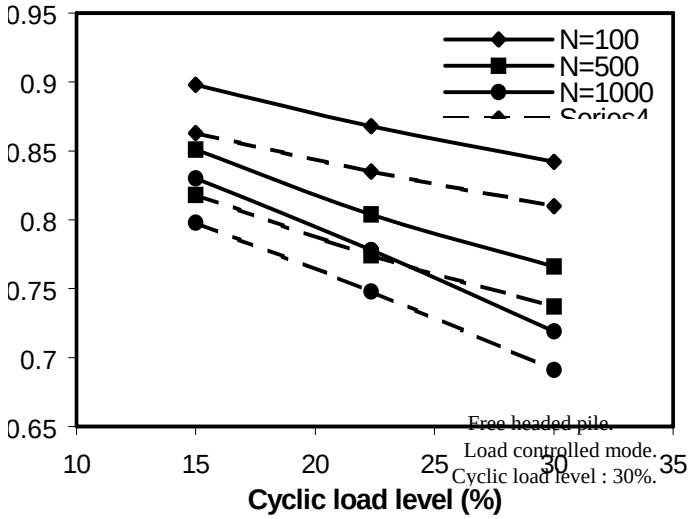

Figure 8. Typical variation of degradation factor with frequency

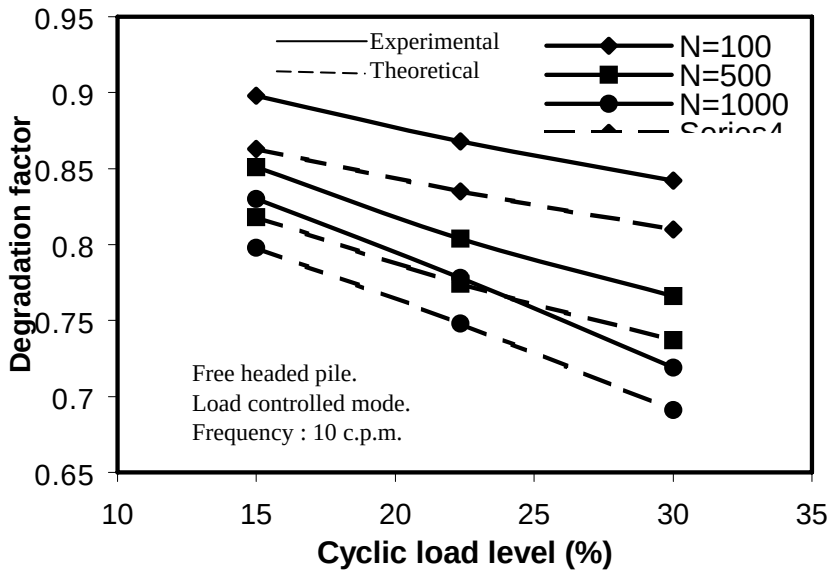

Figure 9. Typical variation of degradation factor with cyclic load level

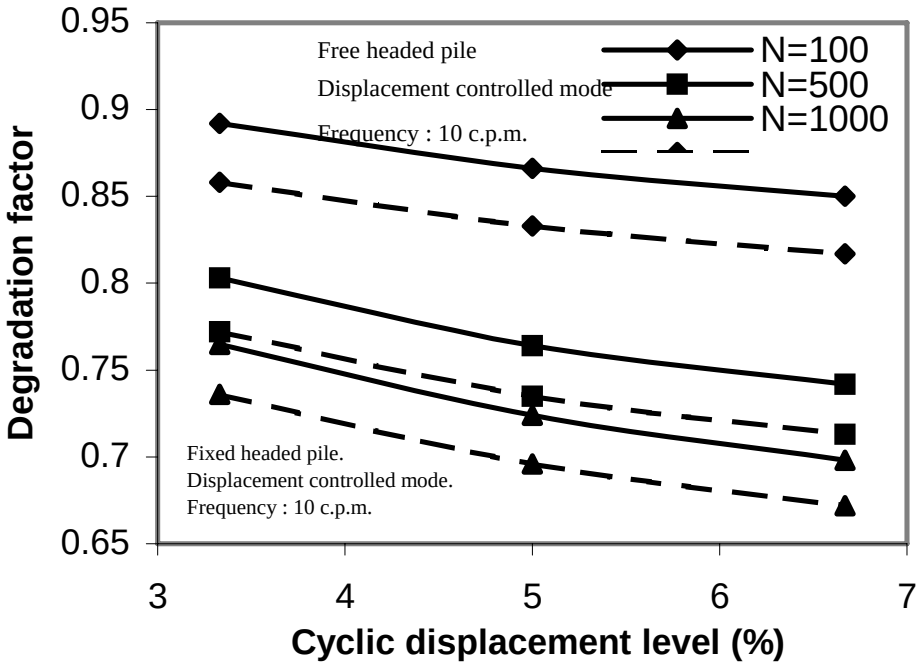

Figure 10. Typical variation of degradation factor with cyclic displacement level.

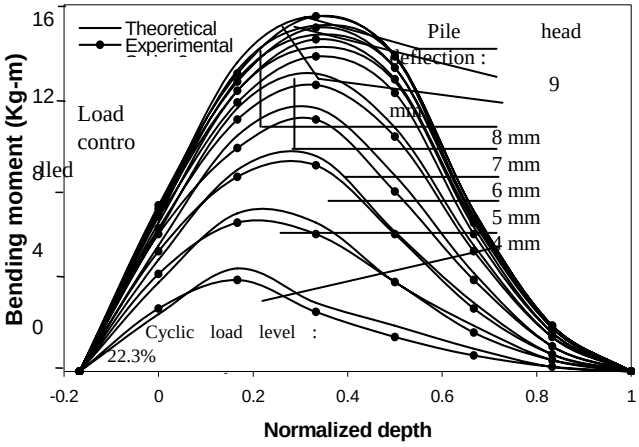

(a)

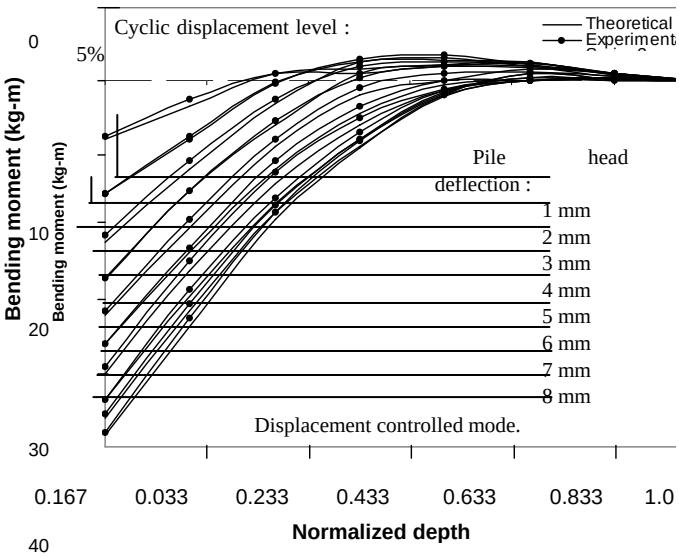

(b)

Figure 11. Bending moment diagram under incremental post cyclic lateral loading of (a) free headed pile. (b) fixed headed pile.

6. CONCLUSIONS

For understanding the behaviour of single pile in marine clay under lateral cyclic loading, a series of experiments under controlled conditions are carried out. Simultaneously, rigorous theoretical analysis based on finite difference technique is done. The results obtained are interpreted rationally to arrive at the following conclusions :

- Excellent agreement between the experimental and the theoretical results are noted. This ensures the validity of the theory.

- To ascertain the deterioration of the pile-soil interactive response under lateral cyclic loading, a term degradation factor is introduced, which is defined as the ratio of post-cyclic to pre-cyclic ultimate lateral pile capacities.
- The average variation between the experimental and theoretical degradation factors is about 4%, the experimental values being on the higher side.
- The load-deflection curves are nearly hyperbolic, the load being stabilized to its optimum value with the head deflection of about 25% to 35% pile diameter.
- The degradation factor decreases with number of cycles and increases with frequency, both asymptotically. Also, the variation of this degradation factor with cyclic load level and cyclic displacement level are non-linear but not asymptotic.
- The basic nature of the theoretical and experimental bending moment diagrams are almost similar. Also, the average variation of the absolute theoretical and experimental maximum bending moments lies between 1-5%, the theoretical value being on the higher side.

Acknowledgement: The authors gratefully acknowledge the financial supports received from All India Council for Technical Education and Council of Scientific and Industrial Research, India to carry out the entire investigation.

REFERENCES

1. Matlock, H., Correlations for Design of Laterally Loaded Piles in Soft Clay., 2nd Annual Offshore Tech. Conf., Houston, **1**(1970) 577-594.
2. Idriss, I.M., Singh, R.D. and Dobry, R., Non-Linear Behaviour of Soft Clay During Cyclic Load. *Journal of Geotechnical Engineering*, *ASCE*, No. 12, **104**(1978) 1427-1447.
3. Poulos, H.G, Behaviour of Laterally Loaded Piles: I - Single Piles, *Journal of Soil Mechanics and Foundation Division, ASCE*, No. 5, **97**(1971) 711-731.
4. Vucetic, M. and Dobry, R., Degradation of Marine Clays under Cyclic Loading, *Journal of Geotechnical Engineering*, No. 2, **114**(1988) 133-149.
5. Basak, S., Behaviour of Pile under Lateral Cyclic Load in Marine Clay., Ph.D. Thesis, *Jadavpur University*, Kolkata, India, 1999.
6. Poulos, H.G., Cyclic Axial Response of Single Pile. *Journal of Geotechnical Engineering*, *ASCE*, No. 1, **107**(1981) 41-58.
7. Poulos, H.G., Single Pile Response to Cyclic Lateral Load. *Journal of Geotechnical Engineering*, *ASCE*, No. 3, **108**(1982) 355-375.
8. Mindlin, R.D., Force at a Point in the Interior of a Semi-Infinite solid. Physics 7, 195, 1936.
9. Douglas, D.J. and Davis, E.H., Movement of Buried Footing due to Moment and Horizontal Load and Movement of Anchor Plates, *Geotechnique*, **14**(1964) 115-132.
10. Broms, B.B., Lateral Resistance of Pile in Cohesive Soil. *Journal of Soil Mechanics and Foundation Division, ASCE*, No. 11, **90**(1964) 27-63.

NOTATIONS

A & B: Dimensionless parameters to be determined from CyUT or CyUDSS tests.
α_i: Cyclic strain amplitude at i-th nodal point.
c_u: Half the unconfined compressive strength of clay.
[C]: Square coefficient matrix.
d: External diameter of pile.
D_f : Degradation factor for ultimate lateral pile capacity.
D_i : Combined nodal soil degradation factor for i-th element.
D_{ri} : Rate factor for i-th element.
D_{si} : Nodal degradation factor of soil strength and stiffness i-th element.
{D} : Augment vector.
δ : Length of a typical pile element.
e: Height of the point of application of lateral load above the soil surface.
E_s : Young's modulus of soil.
E_p : Young's modulus of pile material.
f : Frequency of lateral cyclic loading.
F : Dimensionless rate parameters, to be determined by a series of U.U. triaxial tests.
H : Lateral load applied on the pile head.
I_p : Moment of intertia of the pile cross section.
L : Depth of embedment of pile.
λ_i : Nodal strain rate.
λ_d : Datum strain rate.
M : External moment applied at the head of the free headed pile.
N : Number of cycles.
p_i : Lateral soil pressure acting on the i-th element.
p_{iu} : Ultimate lateral soil pressure for i-th element.
{p}: Lateral soil pressure matrix.
ϕ : Angle of friction of soil.
ρ_i : Nodal displacement of i-th element.
ρ_h : Pile head deflection.
t : Degradation parameter.
τ : Time.